Journal of Animal & Plant Sciences, 36(1): 2026, Page: 116-127
ISSN (print): 1018-7081; ISSN (online): 2309-8694
https://doi.org/10.36899/JAPS.2026.1.0010

EFFECTS OF TGF-B3/PDGF-BB-HEPARIN-HYALURONIC ACID HYDROGEL ON RABBIT KNEE OSTEOARTHRITIS

Z.Y. Wang[1], L. Shi[2], W.T. Chen[3] and B. Feng[4*]

[1]Department of Orthopaedic and Reconstructive Surgery, South China Hospital Affiliated to Shenzhen University, Shenzhen 158000, Guangdong, China;
[2]Department of Orthopaedic Surgery, Rehabilitation Hospital Affiliated to National Rehabilitation AIDS Research Center, Beijing 100000, China;
[3]Material Supply Center, Harbin Medical University Cancer Hospital, Harbin 150000, Heilongjiang, China;
[4]Department of Orthopaedic Medicine, Third Affiliated Hospital of Inner Mongolia Medical University, Baotou 014000, Inner Mongolia, China.
[*]Corresponding author's: Email: fengbo00166@yeah.net

ABSTRACT

Current treatments for knee osteoarthritis (KOA) can alleviate symptoms but fail to repair damaged articular cartilage, while long-term use may lead to side effects. This study aimed to investigate the role of transforming growth factor (TGF)-β3-platelet-derived growth factor (PDGF)-B chain homodimer (BB)/heparin-hyaluronic acid (HA) hydrogel in rabbit KOA to achieve effective articular cartilage repair. Methacrylated hyaluronic acid (HAMA) and heparin (HepMA) were synthesized and utilized as matrices to prepare HepMA-HAMA hydrogel microspheres (MSs). Subsequently, the MSs were co-incubated with TGF-β3 and PDGF-BB to fabricate heparin-HA hydrogel MSs loaded with dual growth factors (HepMA-HAMA@DGFs). The drug loading, release , degradation and biocompatibility characteristics of the prepared hydrogel MSs were examined. New Zealand rabbits were utilized as experimental animals, and a KOA rabbit model was established. Physiological saline (Model group), HA (HA group), hydrogel MSs (HepMA-HAMA group and HepMA-HAMA@DGFs group) were injected into the joint cavity. Healthy rabbits served as the control. Behavioral analysis, knee joint histology, and expression differences of matrix metalloproteinase-13 (MMP-13), tissue inhibitor of metalloproteinases-1 (TIMP-1), and vascular endothelial growth factor (VEGF) in knee articular cartilage were calculated.

Results: The MSs exhibited sustained cumulative drug release and *in vitro* degradation. Co-culturing HepMA-HAMA@DGFs MSs with mouse bone marrow mesenchymal stem cells (MSCs) showed minimal changes in cell growth. In rabbits, the model group exhibited increased Lequesne MG scores, upregulated expression of MMP-13 and VEGF in knee articular cartilage, and downregulated expression of TIMP-1 versus Control (P<0.05). HepMA-HAMA and HepMA-HAMA@DGFs groups showed reduced Lequesne MG scores, downregulated expression of MMP-13 and VEGF in knee articular cartilage, and upregulated expression of TIMP-1 versus Model group (P<0.05). Compared with the HepMA-HAMA group, HepMA-HAMA@DGFs group exhibited decreased Lequesne MG scores, downregulated expressions of MMP-13 and VEGF in knee articular cartilage of rabbits, and upregulated expression of TIMP-1 (P<0.05).

Conclusion: These findings indicate that HepMA-HAMA@DGFs hydrogel MSs have favorable drug release properties, degradation performance, and biocompatibility. Furthermore, HepMA-HAMA@DGFs hydrogel MSs can reduce the expression of MMP-13 and VEGF in KOA cartilage of rabbits, increase the expression of TIMP-1, and promote cartilage repair, thereby exerting therapeutic effects in the treatment of KOA in rabbits.

Keywords: TGF-β3-PDGF-BB/heparin-hyaluronic acid hydrogel, knee osteoarthritis, drug release rate, growth factor, cartilage repair

Published first online November 10, 2025 Published final January 20, 2026

INTRODUCTION

Knee osteoarthritis (KOA) is a degenerative joint disease characterized by destruction of articular cartilage. The incidence rate increases with age and is an important factor leading to disability in the elderly (Dong *et al.,* 2023). The pathogenesis of KOA is still unclear, and there are no effective therapeutic drugs available.

Clinical management mainly focuses on symptom relief and slowing down disease progression (Du *et al.,* 2023).

As a kind of anticoagulant, heparin prevents thrombus formation (Lawanprasert *et al.,* 2022). Heparin has anticoagulant properties. Additionally, heparin exhibits anti-inflammatory and antioxidant effects, which may alleviate joint inflammation and cartilage degeneration associated with the progression of osteoarthritis, indicating its potential in osteoarthritis treatment (Baek *et al.,* 2024). Heparin can also promote the regeneration and repair of cartilage, ehancing osteoarthritis symptoms (Meng *et al.,* 2023; Toktarov *et al.,* 2025). Hydrogels can repair cartilage damage in osteoarthritis, owning to the multifunctional characteristics (Zhang *et al.,* 2021). Microfluidic hydrogel microspheres (MSs) have precisely controlled size and structure, possessing excellent biocompatibility, mechanical strength, colloidal stability, and high surface area (Zhao *et al.,* 2021). A novel drug-eluting dressing can provide controlled therapeutic release to accelerate wound healing while maintaining protective barrier functions. A key component, hyaluronic acid (HA), plays critical physiological roles in wound repair processes (Graça *et al.,* 2020). HA can reduce inflammation, promote cartilage repair, and protect joint structures in osteoarthritis (Wee *et al.,* 2022). As a joint protector, HA is applied to treat osteoarthritis as local joint injections and oral supplements (Kim *et al.,* 2022), which provides effective non-surgical treatment option for alleviating disease symptoms. Transforming growth factor (TGF)-β3-platelet-derived growth factor (PDGF)-B chain homodimer (BB) are two growth factor-based drugs adopted for KOA (Meier Bürgisser *et al.,* 2020). TGF-β3 demonstrates therapeutic potential in treating KOA by stimulating chondrocyte proliferation and enhancing extracellular matrix synthesis, facilitating damaged articular cartilage regeneration (Ude *et al.,* 2018). PDGF-BB stimulates chondrocyte growth and matrix synthesis, enhancing the repair capacity of cartilage tissue (Tsubosaka *et al.,* 2021). Sun *et al*. demonstrated that inverse opal microcarriers loaded with PDGF-BB and TGF-β3 enhanced therapeutic efficacy in rat osteoarthritis (Sun *et al.,* 2024). Nevertheless, their effectiveness remains limited (Pearson and Temenoff, 2022).A single growth factor cannot solve multiple mechanisms required for cartilage repair, while traditional hydrogels have limitations in drug delivery and microenvironment regulation (Shah and Mithoefer, 2020). Hence, a hydrogel capable of co-delivering multiple growth factors with superior biocompatibility and sustained-release properties is an ideal material.

In our work, TGF-β3 and PDGF-BB were incorporated into a heparin-HA hydrogel, whose synergistic effects and superior biological properties can facilitate cartilage repair. This work fabricated hydrogel MSs loaded with TGF-β3 and PDGF-BB to assess their physicochemical properties and biocompatibility. Subsequently, a KOA rabbit model was established, and the effects of intra-articular injection of hydrogel MSs loaded with the dual growth factors on cartilage repair in rabbit KOA were analyzed, to explore new therapeutic approaches for KOA and provide references to improve the therapeutic efficacy.

MATERIALS AND METHODS

Preparation of hydrogel MSs loaded with double growth factors: First, 5 g of HA (Sigma-Aldrich, USA) was fully dissolved in 250 mL of deionized water. Under ice bath conditions, 10 mL of 1.04 g/mL methacrylic anhydride (Jiangshun Chemical Technology Co., Ltd., China) and 10 mL of 200 mg/mL NaOH were applied dropwise with stirring overnight. The mixture was then centrifuged to obtain a precipitate, which was subsequently dialyzed against deionized water at 25°C for 72 h to generate purified methacrylated HA (HAMA). Then, 1 g of Hep (Shanghai Aladdin Co., Ltd., China) was fully dissolved in 50 mL of deionized water. Under ice bath conditions, 8 mL of 1.04 g/mL methacrylic anhydride and 6 mL of 200 mg/mL NaOH were applied dropwise with stirring overnight. Then, chilled anhydrous ethanol was applied dropwise, followed by a 2-h incubation at 4°C. Precipitate was resuspended in 5 mL of deionized water, and further dialyzed at 25°C for 72 h to acquire purified methacrylated heparin (HepMA). A mixture of 4 wt% HAMA, 0.4 wt% HepMA, and 0.4 wt% photoinitiator was dispersed in 95 wt% paraffin oil and 5 wt% Span 80, and emulsified using a microfluidic droplet system (Shanghai Nano Technology Co., Ltd., China) to prepare HepMA-HAMA hydrogel MSs. Froze-dried HepMA-HAMA hydrogel MSs (1 mg) were incubated overnight with 300 ng/mL TGF-β3 (purity: ≥95%, Shanghai AbMole Biological Technology Co., Ltd. China) and 300 ng/mL PDGF-BB (MedChemExpress, USA) to obtain the HepMA-HAMA hydrogel MSs loaded with dual growth factors (HepMA-HAMA@DGFs).

Physical and chemical properties analysis of hydrogel MSs: The dispersed HepMA-HAMA hydrogel MSs were observed for morphology and size employing a scanning electron microscope (SEM). Surface elemental analysis of the HepMA-HAMA hydrogel MSs was conducted using X-ray photoelectron spectroscopy (XPS). Then, 3 mg of freeze-dried HepMA-HAMA MSs were dispersed in 1 mL of deionized water. Such dispersion was shaken at 80 rpm at 37°C for 0, 15, 30, 60, and 120 min, and the supernatant was removed. Hydrogel MS weight was compared to the initial weight. HM@DGFs were placed in 1 mL of phosphate-buffered saline (PBS) + 0.1% bovine serum albumin. The samples were shaken at 80 rpm at 37°C for 0, 1, 3, 5, 7, 15, and 30 days. The

supernatant was collected, and concentrations of TGF-β3 and PDGF-BB were measured using an enzyme-linked immunosorbent assay (ELISA) kit (Sigma-Aldrich). Then, 30 mg of HepMA-HAMA@DGFs were placed in 1 mL of PBS + 1,000 U of hyaluronidase. The samples were shaken at 80 rpm at 37°C for 0, 1, 3, 5, 7, 15, 30, and 60 days. Hydrogel MS weight was measured and compared to the initial weight. Mouse-derived bone marrow mesenchymal stem cells (MSCs) (Shanghai Kanglang Biotechnology Co., Ltd. China) were cultured *in vitro* and seeded in Transwell lower chamber. HepMA-HAMA@DGFs were seeded in upper chamber. Following a 48-h incubation, cells were stained with Calcein acetoxymethyl ester/propidium iodide (AM/PI) working solution (Toxin Research Institute, Japan) and incubated at 37°C for 30 min in the dark. Staining was visualized employing a fluorescence microscope (Y-NE68, Nikon, Japan).

Animals and grouping: Fifty healthy New Zealand white rabbits (2.0 to 2.5 kg), with an equal distribution of males and females, were utilized in this study. Animal experiments were approved by the Ethics Committee of Affiliated Hospital of South China Hospital Affiliated to Shenzhen University (Shenzhen, China), complied with the relevant provisions of the Chinese Association for Laboratory Animal Sciences. The experimental design, procedures, and reporting in this study strictly adhered to the ARRIVE guidelines.

KOA model was prepared using the Hulth method (Zhao *et al.,* 2023). A 3% solution of sodium pentobarbital (30 mg/kg) (Sigma-Aldrich, USA) was injected into marginal ear vein for anesthesia. Following induction of deep anesthesia, standard skin preparation, disinfection, and draping were performed. A longitudinal incision was made along the left knee joint space to expose the medial collateral ligament and adjacent soft tissues, which were subsequently transected. The joint capsule was then incised, followed by complete excision of the medial meniscus and transection of both anterior and posterior cruciate ligaments. Successful ligamentous disruption was confirmed by positive drawer test results. Finally, the joint cavity was irrigated, and wound closure was achieved via layered suturing. Postoperatively, rabbits received intramuscular injection of 40,000 U/kg of sodium penicillin for infection prevention, once a day, for 7 days. At six weeks post-surgery, X-ray examination (K-Alpha™, ThermoScientific, China) was performed to evaluate the modeling effect. A single-blind design was implemented throughout the experiment to minimize potential bias. Using a random number table, successfully modeled rabbits were randomly allocated into the Model, HA, HepMA-HAMA, and HepMA-HAMA@DGFs groups, with 10 rabbits in each group. Healthy animals were utilized as Controls. At 3 and 6 weeks after modeling, Model group received intra-articular injection of 1 mL of normal saline, HA group received injection of 1 mL of PBS with HA, the HepMA-HAMA group received 1 mL HepMA-HAMA hydrogel injection, and the HepMA-HAMA@DGFs group received 1 mL of HepMA-HAMA@DGFs hydrogel injection.

Animal behavior examination: The local response of the knee joint, joint mobility, joint swelling, and gait changes in the animals were observed. The Lequesne MG score (Lu *et al.,* 2024) was utilized to classify the knee joint. 1. Knee Joint Reaction: Grade I: no pain response after the knee joint was touched with a cotton swab. Grade II: contraction of the affected limb after the knee joint was touched with a cotton swab. Grade III: spasmodic contraction of the affected limb with mild reaction after the knee joint was touched with a cotton swab. Grade IV: strong contraction of the affected limb with tremors throughout the body after the knee joint was touched with a cotton swab. 2. Limb Action during Running: Grade I: normal limb action with strong ground contact during running. Grade II: slight limp of the affected limb, but with strong ground contact during running. Grade III: obvious limp of the affected limb during walking. Grade IV: inability to walk on the affected limb or touch the ground. 3. Joint Extension: Grade I: extension of the affected joint beyond 90°. Grade II: extension of the affected joint between 45° and 90°. Grade III: extension of the affected joint between 15° and 45°. Grade IV: extension of the affected joint below 15°. 4. Joint Swelling and Bony Markers: Grade I: no swelling of the affected joint and clear bony markers. Grade II: slight swelling of the affected joint with slightly shallow bony markers. Grade III: observable swelling of the affected joint with disappearance of bony markers. Each grade was assigned a score: Grade I (score 0), Grade II (score 1), Grade III (score 2), and Grade IV (score 3). The total score ranged from 0 to 11.

Observation on HE staining of knee cartilage: After six weeks of drug intervention treatment, the experimental animals from each group were euthanized using air embolism. The knee joints were obtained after dissection. An appropriate amount of articular cartilage was taken and processed by fixation, decalcification, and paraffin embedding. Paraffin sections (5 μm) were prepared and deparaffinized with xylene. The tissue sections were then sequentially immersed in a series of alcohol solutions with increasing concentrations. Following 3-min rinsing with distilled water, section staining with hematoxylin lasted for 5 min, rinsed with distilled water for 5 s, immersed in a 1% hydrochloric acid-ethanol solution for 5 s, and washed with running water for 10 min. Finally, sections were stained with 1% eosin for 2 min and rinsed with distilled water for 5 s. Tissue morphology was observed under an optical microscope, and the modified Mankin scoring system (Asjid *et al.,* 2019) was adopted for evaluation. The

modified Mankin scoring system assesses various aspects of cartilage pathology, including cartilage structure, chondrocytes, matrix staining, and tidemark integrity. Higher scores indicate more severe cartilage pathological changes.

Reverse transcription PCR detection: Appropriate amount of cartilage tissue was collected, and total RNA from cartilage tissue was extracted via TRIzol methodology. cDNA was prepared under the instructions of reverse transcription kit (Takara, Japan). The primers utilized for matrix metalloproteinase-13 (MMP-13) were: upstream 5'-TCCTGATGTGGGTGAATACAATG-3', downstream 5'-GCCATCGTGAAGTCTGGTAAAAT-3'. The primers utilized for issue inhibitor of metalloproteinases-1 (TIMP-1) were: upstream 5'-TACACCCCAGTCATGGAAA-3', downstream 5'-CGGCCCGTGATGAGAAACT-3'. The primers utilized for GAPDH were: upstream 5'-AATGGATTTGGACGCATTGGT-3', downstream 5'-TTTGCACTGGTACGTGTTGAT-3'. Reaction system and program for RT fluorescent quantitative polymerase chain reaction (qPCR) were set up under instructions of the polymerase chain reaction (PCR) kit (Takara, Japan). With glyceraldehyde-3-phosphate dehydrogenase (GAPDH) as reference, relative expressions of the target genes MMP-13 and TIMP-1 were detected using the $2^{-\Delta\Delta Ct}$ methodology.

Immunohistochemical detection: The cartilage tissue was fixed in a 4% paraformaldehyde solution for 24 h. Subsequently, 5 µm paraffin sections were prepared, followed by deparaffinization with xylene. Antigen retrieval was performed using a composite digestion solution, incubating at 25°C for 30 min, and washing with PBS. Then, sections were incubated with 3% hydrogen peroxide and goat serum, followed by the addition of a 1:100 dilution of vascular endothelial growth factor (VEGF) primary antibody (Thermo Fisher, USA). Incubation lasted overnight at 4°C, with an extra 30-min incubation at 25°C. Biotinylated goat anti-rabbit secondary antibody and horseradish peroxidase-labeled streptavidin working solution were applied, followed by incubation. 3,3'-Diaminobenzidine chromogenic solution was applied, and the staining results were observed under a light microscope. Positive staining was indicated by brown, tan, or yellow coloration. Counterstaining was performed with hematoxylin for 15 min, followed by immersion in lithium carbonate for 3 s. Tissue dehydration was carried out using a gradient of alcohols, and the sections were mounted with neutral mounting medium.

Statistical analysis: Data analysis and processing were implemented employing SPSS 22.0. Quantitative data with normal distribution were expressed as mean ± standard deviation. Group differences were analyzed by one-way analysis of variance followed by Tukey's multiple comparison test, which controls type I error (false positive) while being suitable for groups with equal or approximately equal sample sizes. $P<0.05$ implied statistically significant.

RESULTS

Physical and chemical properties analysis of hydrogel MSs: Both HAMA and HepMA-HAMA appeared similar in shape and with complete spherical morphology. In **Fig. 1**, the MSs of HAMA and HepMA-HAMA exhibited a single peak distribution of diameters, with average diameters of (231.3±7.9) µm and (258.6±7.1) µm, respectively.

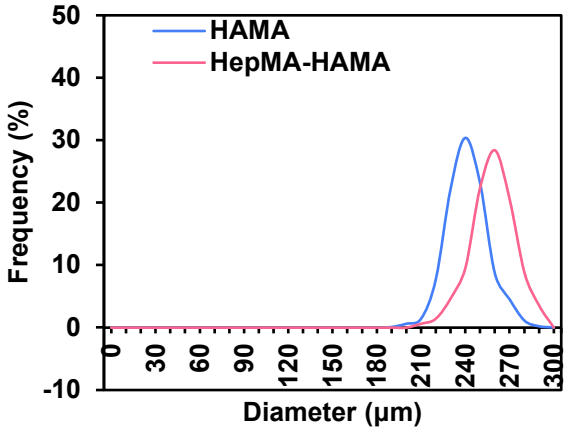

Fig. 1: Morphology and diameter distribution of HAMA and HepMA-HAMA MSs. Both HAMA and HepMA-HAMA MSs exhibited spherical morphology. The diameter of HepMA-HAMA MSs was slightly larger than that of HAMA MSs.

In **Fig. 2A**, HAMA displayed characteristic peaks at 190 eV (Cl 2p), 170 eV (Si 2s), 100 eV (Si 2p), 60 eV (Na 2s), and 50 eV (O 2s). In comparison, HepMA-HAMA exhibited an additional peak at approximately 230 eV (S 2s) and 175 eV (S 2p), indicating the presence of heparin-related sulfur (S) peaks on the HepMA-HAMA hydrogel MSs. In **Fig. 2B**, the swelling ratio of HepMA-HAMA hydrogel MSs in water rapidly increased with incubation time and then slightly decreased. The swelling ratio reached its maximum value (3,053 wt%) after 30 min of incubation and gradually stabilized around 2,800 wt%. In **Fig. 2C**, the loading rates of HepMA-HAMA@DGFs MSs for TGF-β3 and PDGF-BB were (92.2±0.8)% and (95.6±0.09)%, respectively. In **Fig. 2D**, the cumulative release rates of TGF-β3 and PDGF-BB from HepMA-HAMA@DGFs hydrogel MSs gradually increased over time. Even after 30 days, both factors continued to be released, with TGF-β3 exhibiting a higher cumulative release rate than

PDGF-BB. In **Fig.2E**, both HepMA-HAMA and HepMA-HAMA@DGFs hydrogel MSs demonstrated relatively rapid degradation during the initial 15 days, followed by a gradual slowdown.

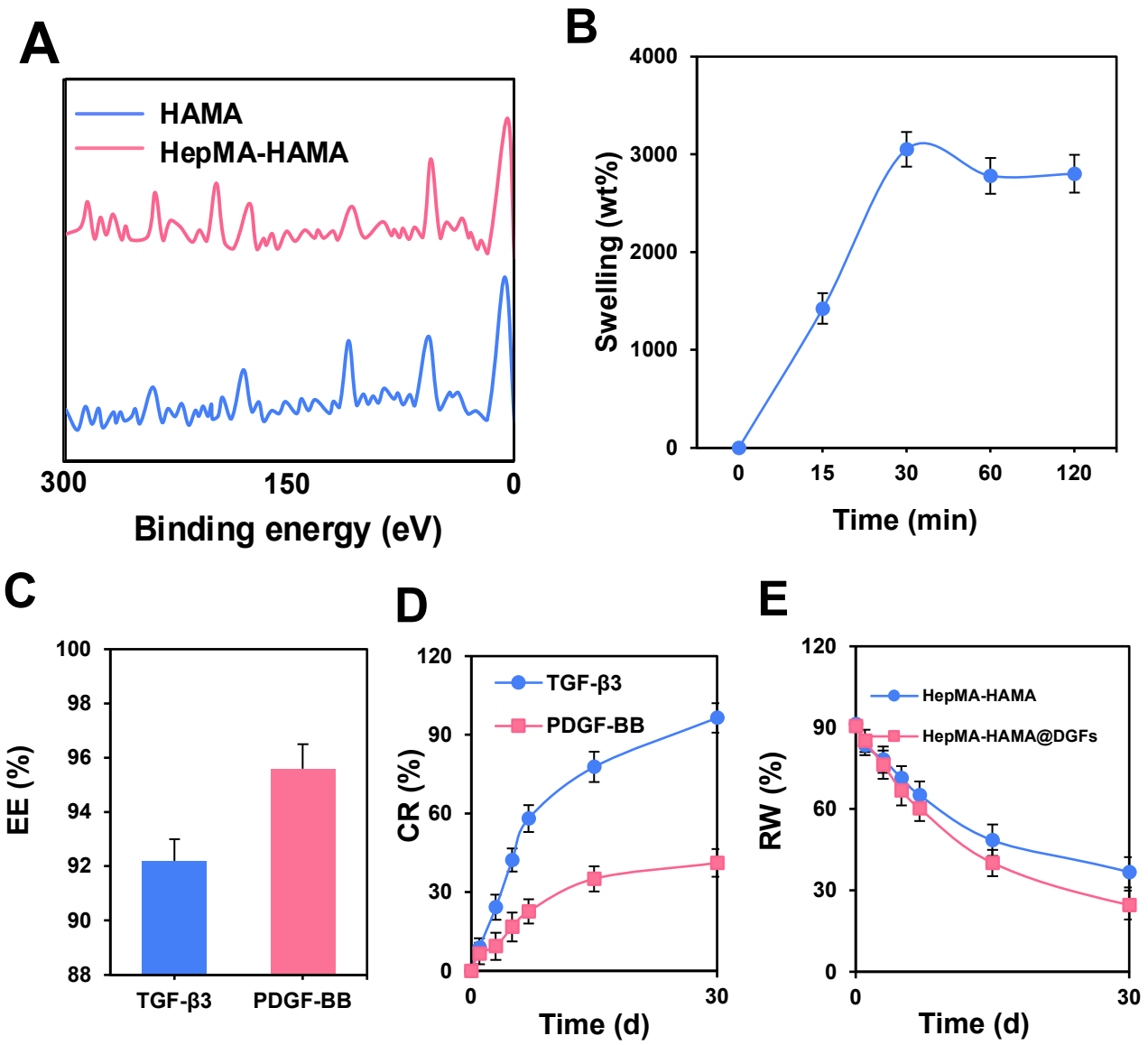

Fig.2: Characterization and properties of HepMA-HAMA hydrogel MSs. A: XPS spectra, showing the emergence of a sulfur (S) peak associated with heparin in HepMA-HAMA versus the characteristic peaks of HAMA; B: swelling curve, indicating that the swelling ratio of HepMA-HAMA hydrogel MSs in water initially increases and then stabilizes over incubation time; C: Encapsulation efficiency, demonstrating the loading capacity of HepMA-HAMA@DGFs MSs for TGF-β3 and PDGF-BB; D: cumulative release profile, showing an increasing trend in the cumulative release of TGF-β3 and PDGF-BB from HepMA-HAMA@DGFs hydrogel MSs over time; E: relative weight change, indicating a gradual decrease in the degradation rate of HepMA-HAMA and HepMA-HAMA@DGFs hydrogel MSs over time.

Biocompatibility analysis of hydrogel MSs: In **Fig.3**, HepMA-HAMA and HepMA-HAMA@DGFs hydrogel MSs were co-cultured with mouse bone marrow MSCs to evaluate their effects on cell growth. It was observed that the number of viable cells greatly increased with culture time in the controls group, HepMA-HAMA group, and HepMA-HAMA@DGFs group. Moreover, the number of viable cells differed slightly among the different groups at 12, 24, 48, and 72 h of culture (P>0.05).

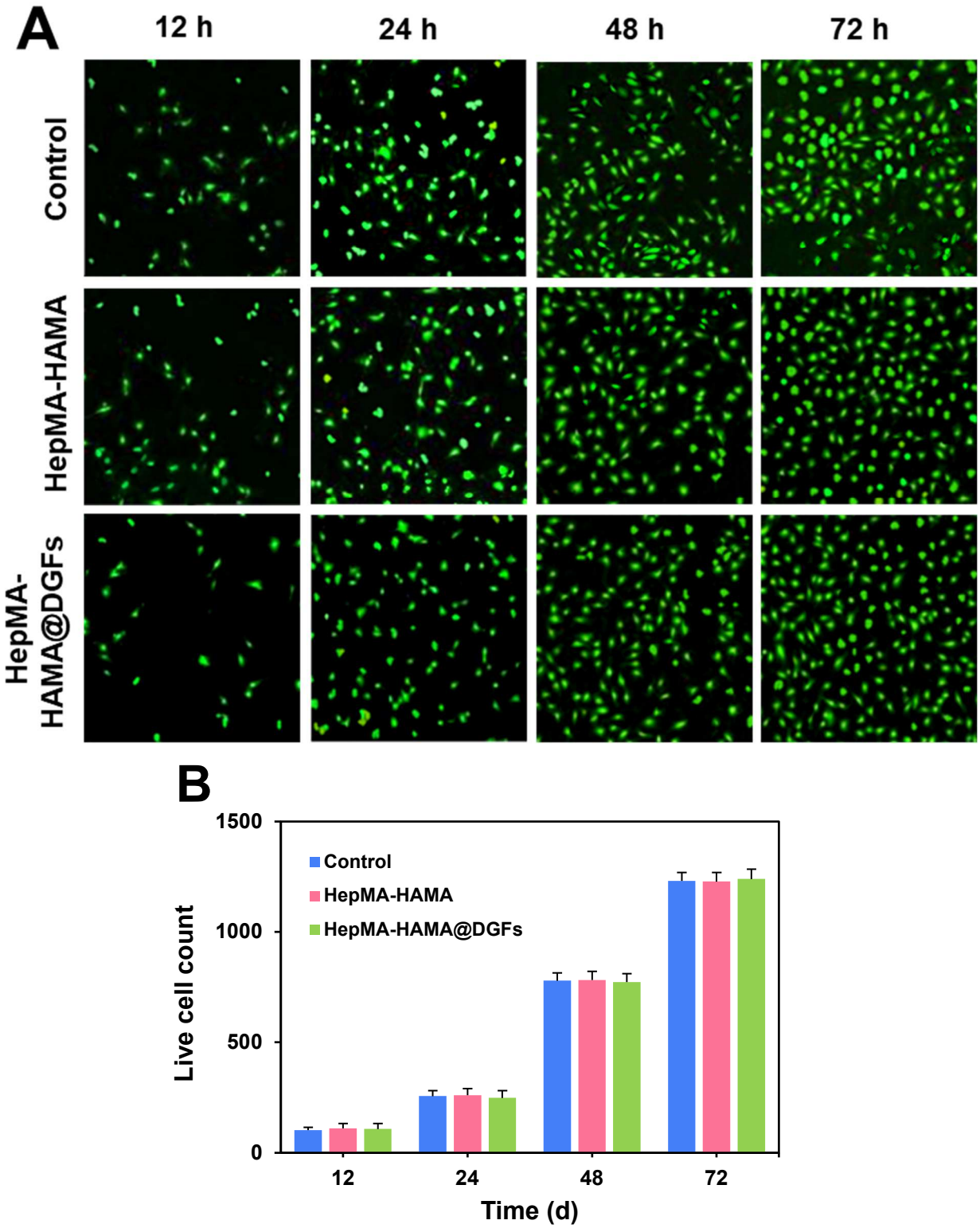

Fig.3: ***In vitro*** **biocompatibility analysis of hydrogel MSs. A: observation of cellular fluorescence staining, scale bar: 400 µm, demonstrating the co-culture of HepMA-HAMA and HepMA-HAMA@DGFs hydrogel MSs with mouse bone marrow MSCs; B: quantification of viable cell count. The number of viable cells significantly increased over the cultivation period in the control, HepMA-HAMA, and HepMA-HAMA@DGFs groups.**

Effect of hydrogel MSs loaded with double growth factors on behavior of KOA: In **Fig.4**, the effects of different therapeutic interventions on behavioral characteristics in a KOA animal model were evaluated using the Lequesne MG score. Statistical analysis was performed using one-way ANOVA followed by Tukey's post hoc test for intergroup comparisons. Considerable differences existed in Lequesne MG scores among the groups (F=15.682, P<0.001). Model group showed a marked increase in the Lequesne MG score versus Controls (P<0.05). Lequesne MG score between Model and HA groups demonstrated negligible differences (P>0.05). HepMA-HAMA and HepMA-HAMA@DGFs groups showed a significant decrease in the Lequesne MG score relative to Model group (P<0.05). Additionally, HepMA-HAMA@DGFs group exhibited a more marked decrease in the Lequesne MG score than HepMA-HAMA group did (P<0.05).

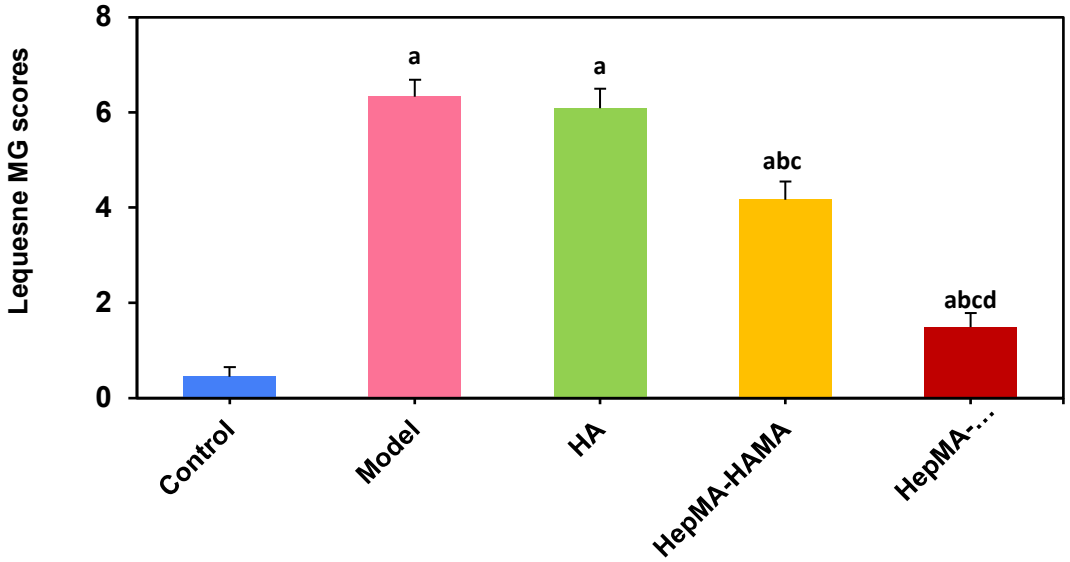

Fig.4: Comparison of Lequesne MG scores among different rabbit groups. Relative to Controls, the Model group exhibited a prominent increase in the Lequesne MG score; both the HepMA-HAMA and HepMA-HAMA@DGFs groups showed lower scores versus Model group. [a]*P*<0.05 vs. Controls; [b]*P*<0.05 vs. Model group; [c]*P*<0.05 vs. HA group; [d]*P*<0.05 vs. HepMA-HAMA group.

Effect of hydrogel MSs loaded with double growth factors on pathological morphology of knee joints: In **Fig. 5**, the effects of various therapeutic interventions on the histopathological features of a KOA animal model were evaluated regarding the Mankin score. One-way ANOVA revealed substantial differences in Mankin scores among the groups (P<0.05). Post hoc analysis using Tukey's test demonstrated that Model group had a more drastic increase in the Mankin score than Controls (P<0.05). Neglectable difference existed in Mankin score between Model and HA groups (P>0.05). Relative to Model group, HepMA-HAMA and HepMA-HAMA@DGFs groups showed a more prominent decrease in the Mankin score (P<0.05). Additionally, HepMA-HAMA@DGFs group exhibited a greater decrease in the Mankin score versus HepMA-HAMA (P<0.05).

Effect of hydrogel MSs loaded with double growth factors in the expression of MMP-13, TIMP-1, and VEGF: In **Fig. 6**, Tukey's test demonstrated that Model group exhibited upregulated MMP-13 mRNA expression (**Fig. 6A**) and downregulated TIMP-1 mRNA expression (**Fig. 6B**) in knee joint cartilage versus Controls (P<0.05). This indicates a close relationship between cartilage damage in KOA and MMPs/TIMPs imbalance. HA group showed no considerable changes in MMP-13 and TIMP-1 mRNA expression in knee joint cartilage relative to Model group (P>0.05). HepMA-HAMA and HepMA-HAMA@DGFs groups exhibited downregulation of MMP-13 mRNA expression and upregulation of TIMP-1 mRNA expression in knee joint cartilage relative to Model group (P<0.05). In **Fig. 6C**, Tukey's test demonstrated that, relative to controls, Model group exhibited a notable increase in VEGF-positive expression (P<0.05). HA group showed slight changes in VEGF-positive expression in knee joint cartilage versus Model group (P>0.05). HepMA-HAMA and HepMA-HAMA@DGFs groups demonstrated a decrease in VEGF-positive expression in knee joint cartilage versus Model group (P<0.05). HepMA-

HAMA@DGFs group exhibited a decrease in VEGF-positive expression in knee joint cartilage relative to HepMA-HAMA group (P<0.05).

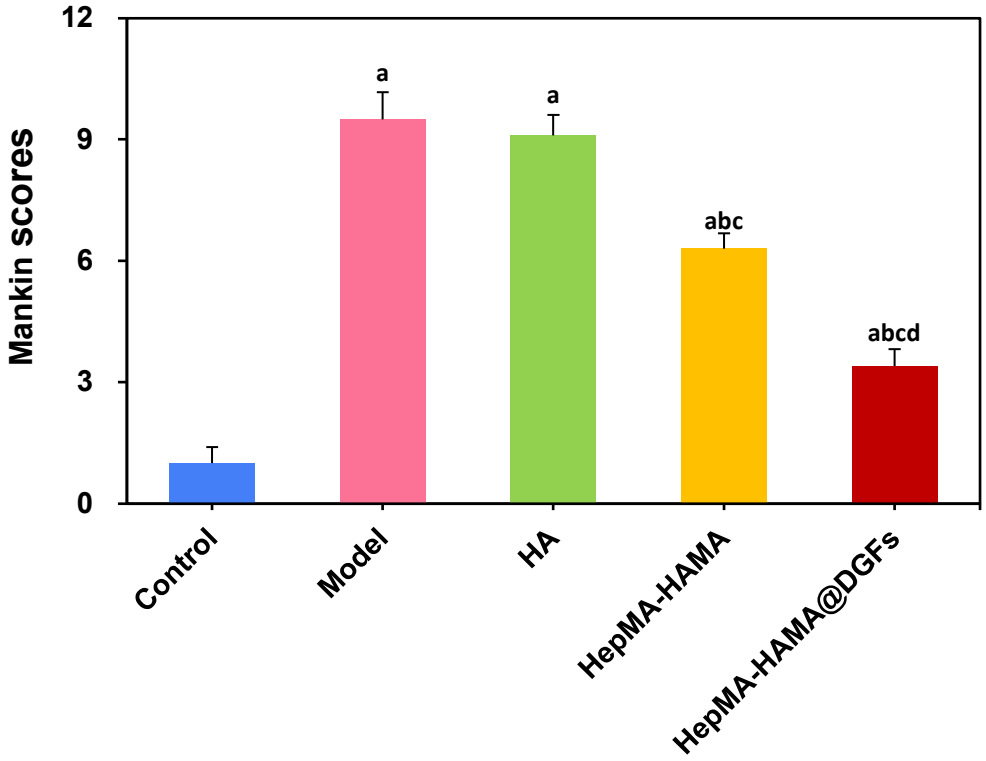

Fig.5: Comparison of Mankin scores among different rabbit groups. Relative to Controls, Model group exhibited a drastic increase in the Mankin score; both the HepMA-HAMA and HepMA-HAMA@DGFs groups showed lower scores versus Model group. [a]P<0.05 vs. controls; [b]P<0.05 vs. Model group; [c]P<0.05 vs. HA group; [d]P<0.05 vs. HepMA-HAMA group.

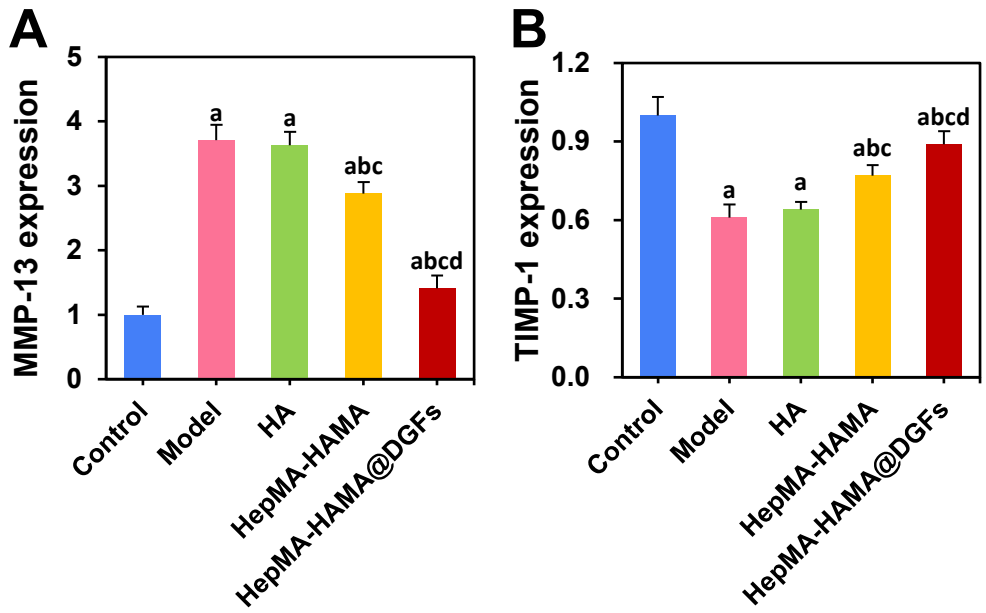

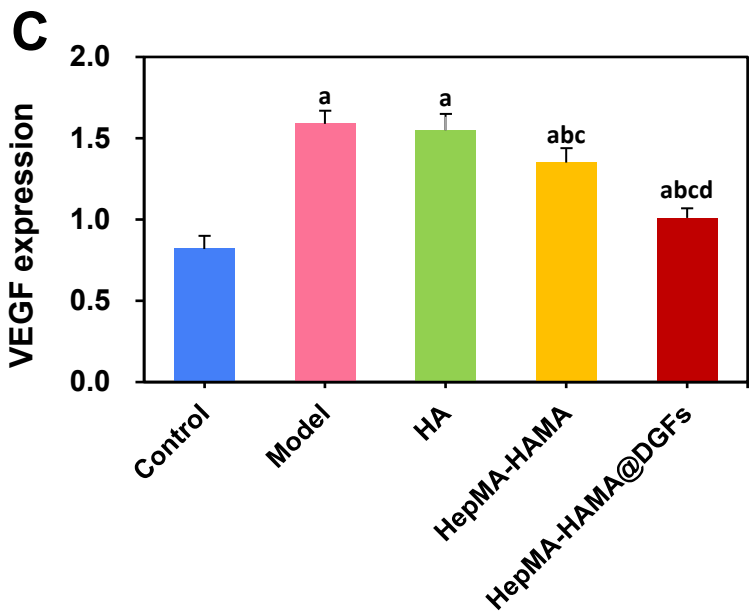

Fig. 6: Comparison of MMP-13, TIMP-1 mRNA, and VEGF expression levels in KOA animals. (A) MMP-13 mRNA: Model group showed upregulation in expression levels versus Controls, while the HepMA-HAMA and HepMA-HAMA@DGFs groups exhibited downregulation relative to the Model group; (B) TIMP-1 mRNA: Model group showed downregulation in expression versus Controls, while the HepMA-HAMA and HepMA-HAMA@DGFs groups demonstrated upregulation relative to the Model group; (C) Quantification of VEGF expression: Model group showed a substantial increase in expression versus Controls, while the HepMA-HAMA and HepMA-HAMA@DGFs groups exhibited reduced expression relative to Model group. [a]*P*<0.05 vs. Controls; [b]*P*<0.05 vs. Model group; [c]*P*<0.05 vs. HA group; [d]*P*<0.05 vs. HepMA-HAMA group.

DISCUSSION

This study explored the pharmacological mechanism of TGF-β3-PDGF-BB/heparin-HA hydrogel on KOA in rabbits. The experiments showed that the heparin-HA hydrogel exhibited marked anti-inflammatory effects in the rabbit KOA model. TGF-β3-PDGF-BB/heparin-HA hydrogel reduced joint swelling and pain and decreased inflammatory mediator release. Such hydrogel helps restore the structure and function of damaged joint cartilage.

Lequesne MG score comparison pre- and post-treatment can evaluate the improvement in knee joint function and quality of life (Silvestre *et al.,* 2023; Saiz *et al.,* 2023). In our study, TGF-β3-PDGF-BB/heparin-HA hydrogel (HepMA-HAMA@DGFs) treatment showed lowered Lequesne MG score in the rabbit KOA model and modulated MMP-13, VEGF, and TIMP-1 levels. It was reported that TGF-β3 is vital in promoting chondrocyte proliferation and differentiation, while PDGF-BB promotes cartilage regeneration and repair (Zhou *et al.,* 2017; Ji *et al.,* 2020). MMP-13 can break down type II collagen in the cartilage matrix, leading to cartilage destruction (Hu and Ecker, 2021). VEGF promotes the formation of new blood vessels, causing infiltration of inflammatory cells and cartilage damage (Le *et al.,* 2021). High VEGF level is related to the severity of joint inflammation and pain. TIMP-1 can inhibit activity of MMPs, reducing cartilage matrix degradation and protecting cartilage (Zahran *et al.,* 2024). Elevated TIMP-1 level may become a potential therapeutic strategy to protect cartilage tissue by inhibiting overactive MMPs (Haraden *et al.,* 2019; Hsueh *et al.,* 2021). Prolonged expression of TGF-β3/BMP-6 could improve joint cartilage formation and restore the zonal structure (Lu *et al.,* 2014). Huang *et al.* stated that TGF-β3 plus BMP-6 could promote joint cartilage regeneration (Huang *et al.,* 2020). Liu *et al.* reported that TGF-β3 promotes the production of cartilage growth factors (Liu *et al.,* 2023). PDGF-BB is involved in cell proliferation, migration, and differentiation, acts crucially in bone regeneration, and promotes new bone formation by stimulating proliferation of osteoblasts (Lv *et al.,* 2023). Additionally, PDGF-BB can enhance osteoblast activity, increase bone matrix deposition, and thereby accelerate fracture healing and bone tissue regeneration (Mihaylova *et al.,* 2018). Chen *et al.* and Younesi *et al.* both stated that PDGF-BB could improve the results of flexor tendon repair surgery (Chen *et al.,* 2022; Younesi *et al.,* 2017). Although previous studies have shown that

TGF-β3 and PDGF-BB each have positive effects on cartilage repair, this study is the first to combine the two in a heparin-HA hydrogel and systematically evaluate their effectiveness in KOA treatment through both in vitro and in vivo experiments. Through this combination, we not only confirmed their synergistic effect on cartilage repair but also provided a new localized delivery system to enhance the efficacy of growth factors, filling a gap in the existing literature regarding the synergistic effects and delivery systems of multiple growth factors.

This study indicates that the HepMA-HAMA@DGFs hydrogel exerts considerable cartilage protection and repair effects by regulating expressions of MMP-13, VEGF, and TIMP-1. This is closely related to theories in tissue engineering and regenerative medicine, extracellular matrix regulation, and signal transduction. This study validates the significance of biomaterials in tissue engineering. Heparin-HA hydrogel can stably release growth factors, thereby enhancing their bioactivity and efficacy. This echoes the theory in tissue engineering that 3D scaffold materials are important for cell proliferation, differentiation, and tissue regeneration (Qu *et al.,* 2021). It was found that TGF-β3 and PDGF-BB can promote cartilage repair by regulating MMP-13 and TIMP-1 expression. This supports the extracellular matrix regulation theory in cartilage regeneration, that is, the dynamic balance of ECM components is critical to maintaining cartilage tissue structure and function (Statham *et al.,* 2022). These findings further validate the key role of signal transduction in cell growth, differentiation, and tissue repair, suggesting that more effective tissue regeneration can be achieved through multiple signaling pathways (Li *et al.,* 2023). By integrating these results and theories, this study validates the effectiveness of existing theories and provides new experimental data and insights, providing optimized treatment methods for KOA.

Nevertheless, this study has certain limitations. First, only a rabbit model was utilized in this experiment, translation to human KOA treatment may face challenges due to interspecies physiological differences, and safety and efficacy assessment in human application is required. Second, the short duration precluded comprehensive evaluation of long-term therapeutic effects. Future studies will include clinical trials to assess the feasibility and efficacy of this hydrogel in human KOA treatment, along with extended observation periods to investigate its long-term impact on articular cartilage repair and related parameters.

Conclusion: The HAMA and HepMA composite hydrogel microspheres loaded with TGF-β3 and PDGF-BB (HepMA–HAMA@DGFs) exhibit favorable drug release, degradation properties, and biocompatibility. They reduce the expression of MMP-13 and VEGF in the articular cartilage of rabbit KOA, while increasing the expression of TIMP-1. This leads to attenuated release of inflammatory factors, alleviation of joint swelling and pain, and promotion of structural and functional recovery of damaged articular cartilage. These findings provide an important basis for the development of KOA treatment strategies and the investigation of its pathogenesis. In the future, this growth factor-loaded hydrogel microsphere-based therapeutic strategy holds promise as a potential effective approach for the clinical treatment of KOA and offers new insights for the treatment of other joint diseases.

Author's contribution: Conception and study design: Zhiyu Wang and Bo Feng; data acquisition and analysis: Lei Shi and Weitong Chen; manuscript draft, editing and revision: Zhiyu Wang and Bo Feng. All authors approved the final manuscript.

Competing Interest: The authors have declared that no competing interest exists.

REFERENCES

Asjid, R., T. Faisal, K. Qamar, S. Malik, F. Umbreen and M. Fatima (2019). Effect of Platelet-rich Plasma on Mankin Scoring in Chemically-induced Animal Model of Osteoarthritis. J Coll Physicians Surg Pakistan 29:1067-1071. https://doi.org/10.29271/jcpsp.2019.11.1067

Baek, J. H., S. C. Lee, D. N. Lee, H. S. Ahn and C. H. Nam (2024). Effectiveness and Complications of Bone Marrow Aspirate Concentrate in Patients with Knee Osteoarthritis of Kellgren-Lawrence Grades II-III. Medicina (Kaunas). 60(6): 977. https://doi.org/10.3390/medicina60060977

Chen, Y., L. Jiang, K. Lyu, J. Lu, L. Long, X. Wang, T. Liu and S. Li (2022). A Promising Candidate in Tendon Healing Events-PDGF-BB. Biomolecules. 12:1518. https://doi.org/10.3390/biom12101518

Dong, Y., Y. Yan, J. Zhou, Q. Zhou and H. Wei (2023). Evidence on risk factors for knee osteoarthritis in middle-older aged: a systematic review and meta analysis. J Orthop Surg Res. 18:634. https://doi.org/10.1186/s13018-023-04089-6

Du, X., Z.Y. Liu, X.X. Tao, Y.L. Mei, D.Q. Zhou, K. Cheng, S.L. Gao, H.Y. Shi, C. Song and X.M. Zhang (2023). Research Progress on the Pathogenesis of Knee Osteoarthritis. Orthop Surg. 15: 2213–2224. https://doi.org/10.1111/os.13809

Graça, M.F.P., S.P. Miguel, C.S.D. Cabral and I.J. Correia (2020). Hyaluronic acid-Based wound dressings: A review. Carbohydr Polym. 241:116364. https://doi.org/10.1016/j.carbpol.2020.116364

Haraden, C.A., J.L. Huebner, M.F. Hsueh, Y.J. Li and V.B. Kraus (2019). Synovial fluid biomarkers

associated with osteoarthritis severity reflect macrophage and neutrophil related inflammation. Arthritis Res Ther. 21:146. https://doi.org/10.1186/s13075-019-1923-x

Hsueh, M.F., X. Zhang, S.S. Wellman, M.P. Bolognesi and V.B. Kraus (2021). Synergistic Roles of Macrophages and Neutrophils in Osteoarthritis Progression. Arthritis Rheumatol. 73:89-99. https://doi.org/10.1002/art.41486

Hu, Q. and M. Ecker (2021). Overview of MMP-13 as a Promising Target for the Treatment of Osteoarthritis. Int J Mol Sci. 22:1742. https://doi.org/10.3390/ijms22041742

Huang, Y., D. Seitz, Y. Chevalier, P.E. Müller, V. Jansson and R.M. Klar (2020). Synergistic interaction of hTGF-β3 with hBMP-6 promotes articular cartilage formation in chitosan scaffolds with hADSCs: implications for regenerative medicine. BMC Biotechnol. 20:48. https://doi.org/10.1186/s12896-020-00641-y

Ji, X., Z. Lei, M. Yuan, H. Zhu, X. Yuan, W. Liu, H. Pu, J. Jiang, Y. Zhang, X. Jiang and J. Xiao (2020). Cartilage repair mediated by thermosensitive photocrosslinkable TGFβ1-loaded GM-HPCH via immunomodulating macrophages, recruiting MSCs and promoting chondrogenesis. Theranostics. 10:2872-2887. https://doi.org/10.7150/thno.41622

Kim, P., J. Park, D.J. Lee, S. Mizuno, M. Shinohara, C.P. Hong, Y. Jeong, R. Yun, H. Park, S. Park, K.M. Yang, M.J. Lee, S.P. Jang, H.Y. Kim, S.J. Lee, S.U. Song, K.S. Park, M. Tanaka, H. Ohshima, J.W. Cho, F. Sugiyama, S. Takahashi, H.S. Jung and S.J. Kim (2022). Mast4 determines the cell fate of MSCs for bone and cartilage development. Nat Commun. 13:3960. https://doi.org/10.1038/s41467-022-31697-3

Lawanprasert, A., S. Pimcharoen, S. E. Sumner, C. T. Watson, K. B. Manning, G. S. Kirimanjeswara and S. H. Medina (2022). Heparin-Peptide Nanogranules for Thrombosis-Actuated Anticoagulation. Small. 18(46): e2203751. https://doi.org/10.1002/smll.202203751

Le, X., M. Nilsson, J. Goldman, M. Reck, K. Nakagawa, T. Kato, L.P. Ares, B. Frimodt-Moller, K. Wolff, C. Visseren-Grul, J.V. Heymach and E.B. Garon (2021). Dual EGFR-VEGF Pathway Inhibition: A Promising Strategy for Patients With EGFR-Mutant NSCLC. J Thorac Oncol. 16:205-215. https://doi.org/ 10.1016/j.jtho.2020.10.006

Li, C., P. Wei, L. Wang, Q. Wang, H. Wang and Y. Zhang (2023). Integrated Analysis of Transcriptome Changes in Osteoarthritis: Gene Expression, Pathways and Alternative Splicing. Cartilage. 14:235-246. https://doi.org/10.1177/19476035231154511

Liu, H., P.E. Müller, A. Aszódi and R.M. Klar (2023). Osteochondrogenesis by TGF-β3, BMP-2 and noggin growth factor combinations in an ex vivo muscle tissue model: Temporal function changes affecting tissue morphogenesis. Front Bioeng Biotechnol. 11:1140118. https://doi.org/10.3389/fbioe.2023.1140118

Lu, C.H., T.S. Yeh, C.L. Yeh, Y.H. Fang, L.Y. Sung, S.Y. Lin, T.C. Yen, Y.H. Chang and Y.C. Hu (2014). Regenerating cartilages by engineered ASCs: prolonged TGF-β3/BMP-6 expression improved articular cartilage formation and restored zonal structure. Mol Ther. 22:186-95. https://doi.org/10.1038/mt.2013.165

Lu, M., D.H. Meng, Z.Y. She, X. Wu, S. Xia, K.N. Yang, C.B. Liu, T. Li and Y.H. Yang (2024). Promotion and Mechanism of Acupotomy on Chondrocyte Autophagy in Knee Osteoarthritis Rabbits. Chin J Integr Med. 30(9):809-817. https://doi.org/10.1007/s11655-024-3759-8

Lv, Z., T. Hu, Y. Bian, G. Wang, Z. Wu, H. Li, X. Liu, S. Yang, C. Tan, R. Liang and X. Weng, (2023). A MgFe-LDH Nanosheet-Incorporated Smart Thermo-Responsive Hydrogel with Controllable Growth Factor Releasing Capability for Bone Regeneration. Adv Mater. 35(5): e2206545. https://doi.org/10.1002/adma.202206545

Meier Bürgisser, G., O. Evrova, M. Calcagni, C. Scalera, P. Giovanoli and J. Buschmann (2020). Impact of PDGF-BB on cellular distribution and extracellular matrix in the healing rabbit Achilles tendon three weeks post-operation. FEBS Open Bio. 10:327-337. https://doi.org/10.1002/2211-5463.12736

Meng, J., W. Liu, Y. Xiao, H. Tang, Y. Wu and S. Gao (2023). The role of aspirin versus low-molecular-weight heparin for venous thromboembolism prophylaxis after total knee arthroplasty: a meta-analysis of randomized controlled trials. Int J Surg. 109:3648-3655. https://doi.org/10.1097/JS9.0000000000000656

Mihaylova, Z., R. Tsikandelova, P. Sanimirov, N. Gateva, V. Mitev and N. Ishkitiev (2018). Role of PDGF-BB in proliferation, differentiation and maintaining stem cell properties of PDL cells in vitro. Arch Oral Biol. 85:1-9. https://doi.org/ 10.1016/j.archoralbio.2017.09.019

Pearson, J.J. and J.S. Temenoff (2022). Growth Factor Immobilization Strategies for Musculoskeletal Disorders. Curr Osteoporos Rep. 20:13-25. https://doi.org/10.1007/s11914-022-00718-x

Qu, M., C. Wang, X. Zhou, A. Libanori, X. Jiang, W. Xu, S. Zhu, Q. Chen, W. Sun and A. Khademhosseini (2021). Multi-Dimensional Printing for Bone Tissue Engineering. Adv Healthc Mater. 10: e2001986. https://doi.org/

10.1002/adhm.202001986

Saiz, L.C., J. Erviti, L. Leache and M. Gutiérrez-Valencia (2023). Restoring Study PRGF: a randomized clinical trial on plasma rich in growth factors for knee osteoarthritis. Trials. 24:37. https://doi.org/10.1186/s13063-022-07049-3

Shah, S. S., and K. Mithoefer (2020). Current Applications of Growth Factors for Knee Cartilage Repair and Osteoarthritis Treatment. Curr Rev Musculoskelet Med. 13(6): 641–650. https://doi.org/10.1007/s12178-020-09664-6

Silvestre, A., P.F. Lintingre, L. Pesquer, P. Meyer, M.H. Moreau-Durieux and B. Dallaudiére (2023). Retrospective Analysis of Responders and Impaired Patients with Knee Osteoarthritis Treated with Two Consecutive Injections of Very Pure Platelet-Rich Plasma (PRP). Bioengineering (Basel). 10:922. https://doi.org/ 10.3390/bioengineering10080922

Statham, P., E. Jones, L.M. Jennings and H.L. Fermor (2022). Reproducing the Biomechanical Environment of the Chondrocyte for Cartilage Tissue Engineering. Tissue Eng Part B Rev. 28:405-420. https://doi.org/10.1089/ten.TEB.2020.0373

Sun, L., J. Gan, L. Cai, F. Bian, W. Xu and Y. Zhao (2024). Multifunctional inverse opal microcarriers ‐ based cytokines delivery system with stem cell homing capability for osteoarthritis treatment. Aggregate. 5(4): e537. https://doi.org/10.1002/agt2.537

Toktarov, T., Y. Raimagambetov, B. Balbossynov, D. Saginova, M. Abilmazhinov and V. Ogay (2025). Implantation of Heparin-Conjugated Fibrin Hydrogel for Local Defects of Cartilage in Knee Osteoarthritis: A Case Report. Int Med Case Rep J. 18:151-156. https://doi.org/10.2147/IMCRJ.S483485

Tsubosaka, M., M. Maruyama, E.E. Huang, N. Zhang, T. Utsunomiya, Q. Gao, H. Shen, X. Li, J. Kushioka, H. Hirata, Z. Yao, Y.P. Yang and S.B. Goodman (2021). Effect on Osteogenic Differentiation of Genetically Modified IL4 or PDGF-BB Over-Expressing and IL4-PDGF-BB Co-Over-Expressing Bone Marrow-Derived Mesenchymal Stromal Cells In Vitro. Bioengineering (Basel). 8:165. https://doi.org/10.3390/bioengineering8110165

Ude, C. C., B. S. Shamsul, M. H. Ng, H. C. Chen, H. Ohnmar, S. N. Amaramalar, A. R. Rizal, A. Johan, M. Y. Norhamdan, M. Azizi, B. S. Aminuddin and B. H. I. Ruszymah (2018). Long-term evaluation of osteoarthritis sheep knee, treated with TGF-β3 and BMP-6 induced multipotent stem cells. Exp Geronto. 104: 43–51. https://doi.org/10.1016/j.exger.2018.01.020

Wee, A.S., C.K. Lim, S.L. Tan, T.S. Ahmad and T. Kamarul (2022). TGF-β1 and-β3 for Mesenchymal Stem Cells Chondrogenic Differentiation on Poly (Vinyl Alcohol)-Chitosan-Poly (Ethylene Glycol) Scaffold. Tissue Eng Part C Methods. 28:501-510. https://doi.org/10.1089/ten.TEC.2022.0112

Younesi, M., D.M. Knapik, J. Cumsky, B.O. Donmez, P. He, A. Islam, G. Learn, P. McClellan, M. Bohl, R.J. Gillespie and O. Akkus (2017). Effects of PDGF-BB delivery from heparinized collagen sutures on the healing of lacerated chicken flexor tendon in vivo. Acta Biomater. 63:200-209. https://doi.org/10.1016/j.actbio.2017.09.006

Zahran, E. M., S. A. Mohamad, M. M. Elsayed, M. Hisham, S. A. Maher, U. R. Abdelmohsen, M. Elrehany, S. Y. Desoukey and M. S. Kamel (2024). Ursolic acid inhibits NF-κB signaling and attenuates MMP-9/TIMP-1 in progressive osteoarthritis: a network pharmacology-based analysis. RSC Adv. 14:18296–18310. https://doi.org/10.1039/d4ra02780a

Zhang, F.X., P. Liu, W. Ding, Q.B. Meng, D.H. Su, Q.C. Zhang, R.X. Lian, B.Q. Yu, M.D. Zhao, J. Dong, Y.L. Li and L.B. Jiang (2021). Injectable Mussel-Inspired highly adhesive hydrogel with exosomes for endogenous cell recruitment and cartilage defect regeneration. Biomaterials. 278:121169. https://doi.org/10.1016/j.biomaterials.2021.121169

Zhao, T., S. Wang, W. Liu, J. Shen, Y. Dai, M. Shi, X. Huang, Y. Wei, T. Li, X. Zhang, Z. Xie, N. Wang, D. Qin and Z. Li (2023). Clinical efficacy of Yiqi Yangxue formula on knee osteoarthritis and unraveling therapeutic mechanism through plasma metabolites in rats. Front Genet.14:1096616. https://doi.org/10.3389/fgene.2023.1096616

Zhao, Z., G. Li, H. Ruan, K. Chen, Z. Cai, G. Lu, R. Li, L. Deng, M. Cai and W. Cui (2021). Capturing Magnesium Ions via Microfluidic Hydrogel Microspheres for Promoting Cancellous Bone Regeneration. ACS Nano. 15:13041-13054. https://doi.org/10.1021/acsnano.1c02147

Zhou, T., X. Li, G. Li, T. Tian, S. Lin, S. Shi, J. Liao, X. Cai, Y. Lin (2017). Injectable and thermosensitive TGF-β1-loaded PCEC hydrogel system for in vivo cartilage repair. Sci Rep. 7:10553. https://doi.org/10.1038/s41598-017-11322-w.